

## ASSOCIATION OF 5,5'-DIBROMO-O-CRESOLSULFONPHTHALEIN ANIONS WITH DYE CATIONS IN AQUEOUS SOLUTION

Sergiy Shapovalov

<https://doi.org/10.23939/chcht16.03.387>

**Abstract.** The formation of associates in aqueous solutions between single- or double-charged anions of 5,5'-dibromo-o-cresolsulfonphthalein and single-charged cations of cyanine dyes (quinaldine blue, quinaldine red) has been considered. Based on the spectrophotometric data, the equilibrium constants of the association were analyzed. The energy of cation-anion interactions (standard enthalpy of formation of ions and associates) was determined by the semi-empirical AM1 method and probable structures of associates were set. The consistency between experimental spectrophotometric and calculated quantum chemical data is discussed.

**Keywords:** association, absorption spectra, 5,5'-dibromo-o-cresolsulfonphthalein, dyes, enthalpy of formation, AM1 method.

## 1. Introduction

Sulfonphthaleins have a wide range of applications, ranging from acid-base or metallochromic indicators<sup>1</sup> up to analytical reagents for the spectral quantitative determination of several organic compounds.<sup>2,3</sup> The bromine derivatives attract attention due to favorable specific features, such as stability of protolytic forms, weak dimerization, good diversity of absorption bands of single- and double-charged anions, high contrast of color reactions.<sup>3,4</sup> In particular, they are used in technologies for determining the acidity of natural waters<sup>5-7</sup> and soils,<sup>8-10</sup> and also form the basis of sensitive elements of fiber optic sensors or devices.<sup>11-15</sup> One of the most common areas of application is the use of bromine derivatives as analytical reagents, including the determination of components in biosamples and pharmaceuticals: antiviral,<sup>16</sup> antiseptic,<sup>17,18</sup> bactericidal,<sup>19-21</sup> antitumor,<sup>22</sup> antihypertensive,<sup>23</sup> antitussives<sup>24,25</sup> and others.<sup>26-29</sup>

The effective use of 5,5'-dibromo-o-cresolsulfonphthalein (DBS) in the technologies of recent years is

known. These include sensitive electrochemical DNA biosensors to the antitumor drug;<sup>31</sup> highly efficient extraction of heavy metals from industrial effluents by adsorption on a modified zeolite surface;<sup>32</sup> lysine decarboxylase analysis,<sup>33</sup> adsorption of hydrophobic molecules on the membrane of erythroleukemia cells;<sup>34</sup> evaluation of the properties of serum albumin,<sup>30,35-41</sup> extracellular lactase.<sup>42</sup> It is noteworthy that many applications are based on the formation of ion pairs (associates) between the anionic form of sulfonphthalein and the analyte.<sup>5,10,17-29</sup> In some cases, such associates can be extracted from the aqueous to organic phases.<sup>17,22,27</sup>

Analysis of publications indicates the need for in-depth study of cation-anionic interactions that cause the formation of associates, which include anions ( $\text{HAN}^-$ ,  $\text{An}^{2-}$ ) of DBS. Some facts of the interaction of sulfonphthalein anions with cations ( $\text{Ct}^+$ ) of some dyes (rhodamines, cyanines) have been covered earlier.<sup>43-45</sup> However, the most probable structure of DBS associates and their energy characteristics, in particular, the standard enthalpy of formation ( $\Delta_f H^0$ ), have not been studied. In this report, using the results of spectrophotometric measurements and quantum chemical calculations, we analyzed the cation-anion interactions that lead to the formation of stoichiometric associations between single or double-charged anions of DBS and single-charged cations of polymethine dyes (quinaldine blue,  $\text{QB}^+$  and quinaldine red,  $\text{QR}^+$ ). Note, that these cations have been used previously under the study of the processes of anionic dye association.<sup>44-46</sup>

## 2. Experimental

### 2.1. Materials and equipment

Distilled water was used to prepare the solutions with an electrical conductivity of no more than  $4 \cdot 10^{-6}$  S. Disodium salts of sulfonphthaleins were used: QB was in the form of chloride salt, and QR was in the form of iodide salt (trademark "Sigma", the content of the basic component was not less than 95%). The proper qualification of the chemical purity of the preparations of each of the dyes was verified spectrophotometrically, taking into account the known values of the molar

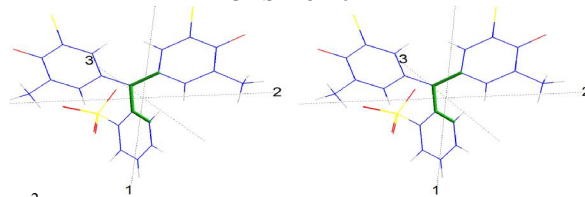
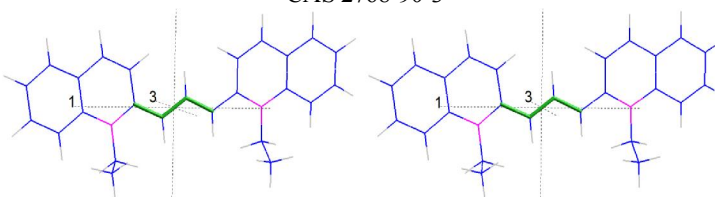
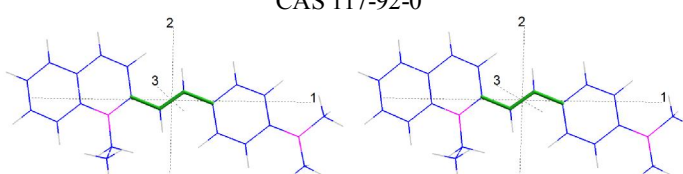
absorption coefficient ( $\epsilon_{\max}$ , L/(mol·cm)) and the maximum absorption band ( $\lambda_{\max}$ ) for the most intensely colored protolytic form. The acidity of the medium was created with phosphate, borate, acetate buffer solutions, and in some cases with hydrochloric acid or sodium hydroxide. Additional observations have shown that the addition of buffer solutions does not significantly affect the light absorption of dyes and association processes. The pH value was monitored with a glass electrode. The ionic strength ( $I$ ) of the solutions did not exceed 0.004. The values of the optical density, which are the basis for the calculations of the equilibrium constants of the association ( $K_{as}$ ), were checked for compliance with the basic law of light absorption. The absorption spectra were measured on upgraded spectrophotometers “Hitachi U3210” or “SF 46” (at room temperature) with an error in determining the absorption wavelength of not less than  $\pm 0.5$  nm. It is experimentally verified that temperature fluctuations within 2–3 degrees have practically no effect on the spectral properties of the studied systems.

## 2.2. Measurements and calculations

Methods of mixtures preparation of dyes and calculation of spectral and equilibrium characteristics of associates are covered by authors.<sup>43,44,46</sup> To calculate the standard formation enthalpies of dye ions and their associates, as well as to establish their structure semi-empirical quantum chemical method AM1 was used. The method is integrated into the software packages “Hyper Chem 8.0” (*evaluation version*) and “MOPAC 2009”. The principles of calculations for the structures of dyes and their ionic associates are described in more detail in publications.<sup>47,48</sup>

When studying the interaction of  $\text{HAn}^-$  (or  $\text{An}^{2-}$ ) with  $\text{Ct}^+$  the acidity of the solution should be observed, which ensures the coexistence of the corresponding protolytic forms (Fig. 1). Otherwise, the interpretation of spectral changes is difficult due to possible interactions involving mixtures of ionic dye forms.

**Table 1.** Spectral, protolytic, and structural characteristics of dyes

Dye	$pK_{a1}$ ( $\lambda_{\max}$ , nm $\text{HAn}^-$ or $\text{Ct}^+$ )	$pK_{a2}$ ( $\lambda_{\max}$ , nm $\text{An}^{2-}$ )
DBS 3,3-bis(3-bromo-4-hydroxy-5-methylphenyl)-3H-2,1 $\lambda^6$ -benzoxathiole-1,1-dione CAS 115-40-2  ( $\text{An}^{2-}$ , torsion angle of rotation of the sulfur is 68.8...71.3°)	-0.75 (431)	6.40 (588)
QB <sup>+</sup> 1-ethyl-2-[3-(1-ethyl-1,2-dihydroquinolin-2-ylidene)prop-1-en-1-yl]quinolin-1-ium chloride CAS 2768-90-3  ( $\text{Ct}^+$ , torsion angle of the marked polymethine bond is 179.0...179.9°)	3.5 (600, $\alpha$ -band; 550, $\beta$ -band)	–
QR <sup>+</sup> 2-(-(4-dimethylamino)styryl)-1-ethylquinolinium iodide CAS 117-92-0  ( $\text{Ct}^+$ , torsion angle of the marked polymethine bond is 177.0...178.4°)	2.63 (528)	–

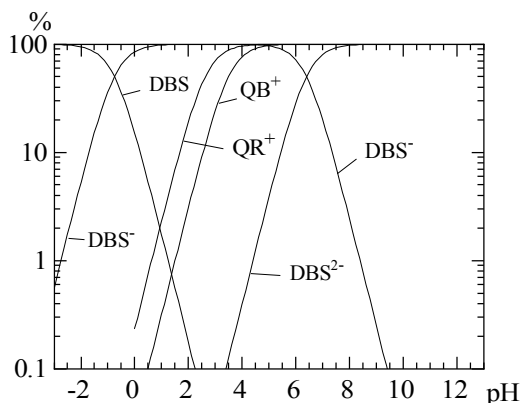


**Fig. 1.** The relative content of protolytic forms of dyes depending on pH of the aqueous solution

Under creating the optimal acidity of the solution, the values of  $pK_{a1}$  and  $pK_{a2}$  were taken into account (see Table 1; the characteristics of DBS ( $pK_{a1}$ ,  $pK_{a2}$ ) and cyanine dyes are given for  $I \rightarrow 0$ ; <sup>46,49,50</sup> the error of  $pK_a$  values is  $\pm (0.03-0.08)$ ; the values of  $pK_{a1}$  for QB and QR refer to the dissociation of  $HCT^{2+}$  cation; the AM1 method was used for determination of the structures geometry; torsion angles are marked with a bold chemical bond; stereo images are given).

For example, the data in Fig. 1 indicate that the interaction of the single-charge anion DBS ( $HAn^-$ ) with  $QB^+$  should be investigated at  $pH = 4.0-5.4$ , and that of the double-charged anion ( $An^{2-}$ ) at  $7.5-9.5$ .

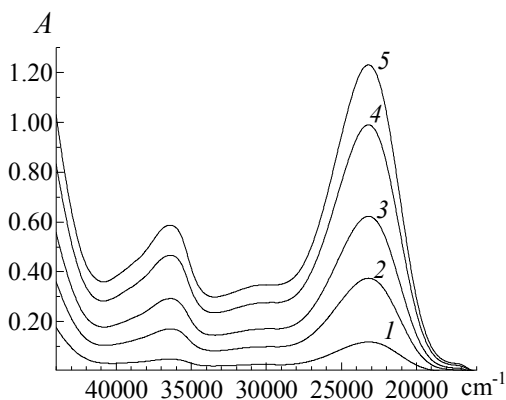


**Fig. 2.** Absorption spectra of aqueous solutions of DBS. Concentrations, mol/L: 1 –  $4.96 \cdot 10^{-6}$ ; 2 –  $1.49 \cdot 10^{-5}$ ; 3 –  $2.48 \cdot 10^{-5}$ ; 4 –  $3.97 \cdot 10^{-5}$ ; 5 –  $4.96 \cdot 10^{-5}$ .  $pH = 4.4$

The correlation coefficient is equal to 0.99995, and its standard deviation is 0.0054. The free term of the regression equation (in parentheses) is a statistical zero. This nature of the dependence obeys the basic law of light absorption and gives reason to believe that in the studied range of concentrations, the single-charge DBS anion is

### 3. Results and discussion

#### 3.1. Protolytic equilibria of dyes in aqueous solutions

Features of DBS and the cyanines are the following: 1) dyes form stable protolytic forms in aqueous solutions; 2) dyes can associate at concentrations not exceeding their solubility in water; 3) ionic forms have a sufficient color intensity and the ability to significantly change the light absorption during association, which allows studying quite small concentrations of interacting particles.

Interpretation of spectral changes from the standpoint of the equilibrium approach (using the law of active masses) implies compliance with the basic law of light absorption by protolytic forms of interacting dyes. The absorption spectra of aqueous DBS solutions were investigated in the concentration range from  $4.96 \cdot 10^{-6}$  to  $4.96 \cdot 10^{-5}$  mol/L using a buffer solution and without the addition of salt additives or organic solvent (Fig. 2, form  $HAn^-$ ). The value of  $I$  did not exceed  $4 \cdot 10^{-4}$ .

Hereinafter, the Savitsky–Goley procedure was used to smooth the electronic spectra.<sup>51,52</sup> The dependence of  $A$  on the DBS molar concentration for  $\lambda_{max} = 431$  nm is shown in Fig. 3. It is a line passing through the origin. The linear regression equation has the form:

$$A_{431} = 0.000488_{(0,00463)} + 24877.3_{(147.8)} \times C_{DBS}$$

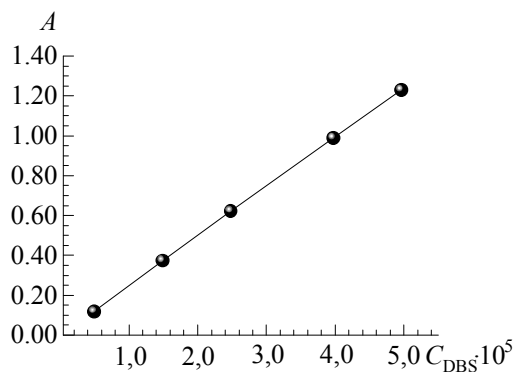


**Fig. 3.** The dependence of the optical density on the molar concentration of DBS at 431 nm

not prone to dimerization. We have experimentally established that this is also applied to the double-charged ion DBS.

Sulfonphthalein molecules are polybasic acids, which are characterized by several protolytic transformations:  $H_3An^+ \rightleftharpoons H_2An^0 \rightleftharpoons HAn^- \rightleftharpoons An^{2-}$ .

Cationic and neutral protolytic forms exist only in a strongly acidic environment. Anions, especially  $\text{An}^{2-}$ , have the most intense color; the light absorption bands of  $\text{HAN}^-$  and  $\text{An}^{2-}$  forms are well spectrally spaced (see, *pl.*,  $\lambda_{\text{max}}$  values with molar absorption coefficients  $\varepsilon_{\text{max}}(\text{HAN}^-) = 24900 \text{ L}/(\text{mol}\cdot\text{cm})$ ,  $\varepsilon_{\text{max}}(\text{An}^{2-}) = 67200 \text{ L}/(\text{mol}\cdot\text{cm})$ ). This contributes to the experimental study of the ionic association of dyes at particle concentrations at the level of  $5 \cdot 10^{-6} \text{ mol/L}$ . It is noteworthy that the coefficient of the linear regression equation practically coincides in value with the given  $\varepsilon_{\text{max}}(\text{HAN}^-)$  (the thickness of the absorbing layer is equal to 1.00 cm, Fig. 2). This indicates that only one protolytic form of DBS exists at a certain acidity of the solution in the aqueous solution. In turn, significant differences in the values of  $\text{p}K_{\text{a}1}$  and  $\text{p}K_{\text{a}2}$  (Table 1) allow regulating the acidity of the solution to create conditions under which the existence of only a single- or double-charged anion is possible.

For QR, the linear regression equation having the form in the concentration range of  $1.0 \cdot 10^{-6} - 1.0 \cdot 10^{-4} \text{ mol/L}$  was defined earlier<sup>46</sup> and has the form:

$$A_{528} = -0.0038_{(0.015)} + 3.37 \cdot 10^4_{(324)} \times C_{\text{QR}}.$$

The correlation coefficient is equal to 0.9996<sub>(0.03)</sub>. Note that the value of the free regression term is statistical zero as in the case of DBS anions.

For QB, in contrast to other dyes, the basic law of light absorption is fulfilled only at relatively low (not more than  $3 \cdot 10^{-6} \text{ mol/L}$ ) concentrations, because QB is very prone to self-association.<sup>43</sup> It is spectrally manifested by a weakening of the absorption of the  $\alpha$ -band and an increase in the intensity of the  $\beta$ -band (Table 1).

Aqueous solutions of single-charged cyanines are markedly discolored due to the processes of protonation (formation of  $\text{HCt}^{2+}$  particles in acidic conditions) and hydrolysis (the occurrence of  $\text{CtOH}$  and the appearance of turbidity in alkaline solutions).

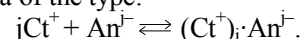
### 3.2. Spectral and equilibrium properties of DBS associates

The most informative idea of changes in light absorption in the systems " $\text{Ct}^+ + \text{HAN}^-$ ", " $\text{Ct}^+ + \text{An}^{2-}$ " is provided by spectral series, which have a fixed concentration of cyanine dye and increase the content of sulfonphthalein. An example of such changes is given in Fig. 4, where a different amount of DBS (curves 2–10) is added to the constant concentration of QB (curve 1). The increase in the concentration of DBS is accompanied by a gradual increase in the optical density of the short-wavelength region of the spectrum (with a band maximum of 431 nm), which is associated with light absorption of the single-charge anion DBS (arrows here and below indicate the change in optical density of the spectral region). The absorption bands  $\text{Ct}^+$  and  $\text{HAN}^-$  are well

spectrally spaced (see  $\lambda_{\text{max}}$  values in Table 1). Note that the absorption intensity of the long-wavelength band  $\text{Ct}^+$  ( $\lambda_{\text{max}} = 600 \text{ nm}$ ) gradually decreases. On the contrary, in the case of the " $\text{Ct}^+ + \text{An}^{2-}$ " system, the absorption bands of the corresponding protolytic forms of dyes are quite close. This prevents the direct perception of spectral shifts and even in such case there is a decrease in the intensity of  $\text{Ct}^+$  absorption (in similar spectral series) if the measurement of the optical density of the solution is not relative to water (Fig. 4), but relative to the solution with the appropriate concentration of DBS (Fig. 5, Fig. 6). Analysis of changes in the electronic absorption spectra of mixtures of  $\text{Ct}^+$  with  $\text{HAN}^-$ ,  $\text{Ct}^+$  with  $\text{An}^{2-}$  leads to the conclusion that the principle of additivity of light absorption is violated. The absorption intensity of the mixture of interacting counterions becomes less than the total light absorption of individual dye ions. This phenomenon is observed regardless of the initial concentrations as  $\text{Ct}^+$  (for example, the initial concentrations of QB are  $4.9 \cdot 10^{-7}$  (Fig. 5),  $4.6 \cdot 10^{-6}$  (Fig. 4),  $4.8 \cdot 10^{-5} \text{ mol/L}$  (Fig. 6), *i.e.* almost 100 times different) and DBS. Such spectral shifts of the absorption bands (in the absence of new bands or splitting of existing bands) suggest a solvate-separated type of associative structure (in accordance with the general features of spectral shifts for dye associate systems).<sup>54</sup>

From the experimental data, it can be concluded that for associates of DBS the stoichiometric ratio of " $\text{QB} : \text{counterion}$ " is 1:1 for the case of the anion  $\text{HAN}^-$ , and is 2:1 for the case of  $\text{An}^{2-}$ .

Taking into account the ratios of stoichiometric coefficients in the associates we determined the association constants ( $K_{\text{as}}$ ) based on the obtained spectral series for equilibria of the type:



The concentration constant of the association  $K_{\text{as}}^{\text{conc.}}$  practically does not differ from the thermodynamic one  $K_{\text{as}}^{\text{thermod.}}$ , because  $I \leq 0.004$  in experiments.

The value of  $K_{\text{as}}$  is calculated by the law of acting masses:

$$K_{\text{as}}^{\text{thermod.}} = K_{\text{as}}^{\text{conc.}} = \frac{[(\text{Ct}^+)_j \cdot \text{An}^{j-}]}{(C_{\text{Ct}^+} - j \times [(\text{Ct}^+)_j \cdot \text{An}^{j-}])^j \times (C_{\text{An}^{j-}} - [(\text{Ct}^+)_j \cdot \text{An}^{j-}])},$$

where  $C_{\text{Ct}^+}$  is the initial molar concentration of the cationic dye (which does not change within the series);  $C_{\text{An}^{j-}}$  is the initial molar concentration of anion;  $[(\text{Ct}^+)_j \cdot \text{An}^{j-}]$  is the equilibrium molar concentration of associate (as), which is calculated based on the principle of additivity of optical density  $A$  of a mixture of colored particles in the solution by the equation:

$$[(\text{Ct}^+)_j \cdot \text{An}^{j-}] = \frac{C_{\text{Ct}^+} \times \varepsilon_{\text{Ct}^+} \times l + C_{\text{An}^{j-}} \times \varepsilon_{\text{An}^{j-}} \times l - A}{(j \times \varepsilon_{\text{Ct}^+} + \varepsilon_{\text{An}^{j-}} - \varepsilon_{\text{as}}) \times l}.$$

An example of the calculation of  $K_{\text{as}}$  for the QB associate is given in Table 2 (values are:  $C_{\text{Ct}^+} =$

$= 4.9 \cdot 10^{-7}$  mol/L,  $\varepsilon_{Ct} = 6.40 \cdot 10^4$  L/(mol·cm),  $\varepsilon_{as} = 5.22 \cdot 10^4$  L/(mol·cm),  $l=5.00$  cm).

The obtained data on the logarithmic values of the association constant (QB:  $6.67 \pm 0.05$  ( $Ct^+ \cdot HAn^-$ ),

$11.07 \pm 0.10$  ( $(Ct^+)_2 \cdot An^{2-}$ ); QR:  $4.78 \pm 0.06$  and  $8.23 \pm 0.04$ , respectively) are in good agreement with the values of  $K_{as}$ , which were defined earlier<sup>46</sup> for slightly different concentration ranges of  $Ct^+$  and DBS.

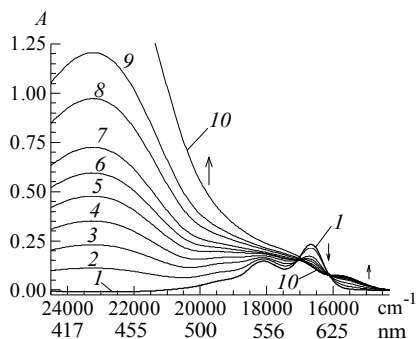


**Fig. 4.** Absorption spectra in the system “DBS + QB”. Concentrations, mol/L, QB:  $4.6 \cdot 10^{-6}$  (1–10); DBS: 0 (1),  $3.0 \cdot 10^{-6}$  (2)... $5.5 \cdot 10^{-5}$  (10). The thickness of the absorbing layer is 1.0 cm. pH = 4.5. Comparison solutions are water

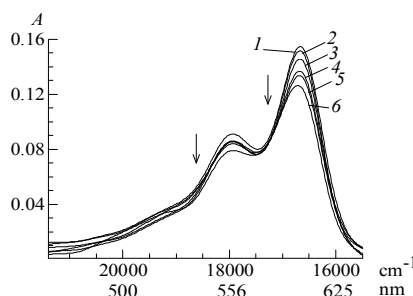


**Fig. 5.** Absorption spectra in the system “DBS + QB”. Concentrations, mol/L, QB:  $4.9 \cdot 10^{-7}$  (1–6); DBS: 0 (1),  $1.00 \cdot 10^{-6}$  (2)... $5.01 \cdot 10^{-5}$  (6). The thickness of the absorbing layer is 5.0 cm, pH = 9.2. Comparison solutions are: water (1); DBS solution at the appropriate concentration (2–6)

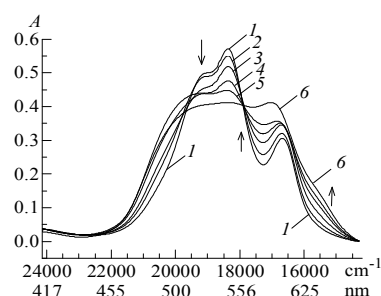


**Fig. 6.** Absorption spectra in the system “DBS + QB”. Concentrations, mol/L, QB:  $4.8 \cdot 10^{-5}$  (1–6); DBS: 0 (1),  $1.01 \cdot 10^{-5}$  (2)... $3.03 \cdot 10^{-5}$  (6). The thickness of the absorbing layer is 0.20 cm, pH = 9.2. Comparison solutions are: water (1); DBS solution at the appropriate concentration (2–6)

**Table 2.** Calculation of  $K_{as}$  for the associate  $(Ct^+)_2 \cdot An^{2-}$

The mixture	$C_{An}$	$A$	$[(Ct^+)_2 \cdot An^{2-}]$	$C_{Ct} - 2 \times [(Ct^+)_2 \cdot An^{2-}]$	$C_{An} - [(Ct^+)_2 \cdot An^{2-}]$	$K_{as}$
1	$5.01 \cdot 10^{-7}$	0.1549	$8.7 \cdot 10^{-9}$	$4.77 \cdot 10^{-7}$	$4.92 \cdot 10^{-7}$	$7.77 \cdot 10^{10}$
2	$1.01 \cdot 10^{-6}$	0.1488	$2.5 \cdot 10^{-8}$	$4.46 \cdot 10^{-7}$	$9.75 \cdot 10^{-7}$	$1.29 \cdot 10^{11}$
3	$2.01 \cdot 10^{-6}$	0.1449	$3.5 \cdot 10^{-8}$	$4.24 \cdot 10^{-7}$	$1.98 \cdot 10^{-6}$	$9.82 \cdot 10^{10}$
4	$2.51 \cdot 10^{-6}$	0.1401	$4.7 \cdot 10^{-8}$	$4.00 \cdot 10^{-7}$	$2.46 \cdot 10^{-6}$	$1.19 \cdot 10^{11}$
5	$3.51 \cdot 10^{-6}$	0.1370	$5.5 \cdot 10^{-8}$	$3.84 \cdot 10^{-7}$	$3.45 \cdot 10^{-6}$	$1.08 \cdot 10^{11}$
6	$4.01 \cdot 10^{-6}$	0.1303	$7.3 \cdot 10^{-8}$	$3.48 \cdot 10^{-7}$	$3.94 \cdot 10^{-6}$	$1.52 \cdot 10^{11}$

It should be noted that turbidity may appear in more concentrated solutions ( $>8.0 \cdot 10^{-5}$  mol/L) of mixtures of dyes. This fact indicates the formation of associates of more complex stoichiometry, which are sparingly soluble in water:  $(Ct^+)_j \cdot An^{2-} + kAn^{2-} \rightleftharpoons (Ct^+)_j \cdot (An^{2-})_{k+1}$ . Thus, it is possible to form associates of complex composition by a cooperative mechanism, when the counterion interacts not only with the dye but with the associate. A similar phenomenon was recorded for tetraphenylborate anion by spectrophotometry<sup>55</sup> and for “daunomycin + ethidium bromide”<sup>56</sup> and “acridine orange + caffeine”<sup>57</sup> by other instrumental methods, such as 1H NMR spectroscopy.

Comparison of the values of  $\lg K_{as}$  (Table 2) shows that the QB associates are more stable than QR associates.<sup>46</sup> This is probably due to the fact that the lower hydrophobicity of QR compared to QB (decimal indexes of hydrophobicity are  $\log P_{QR} = 5.15 \pm 0.12$  and  $\log P_{QB} = 5.69 \pm 0.12$  according to our results)<sup>58</sup> reduces

the manifestation of hydrophobic interactions in QR associates. In addition, the positive charge is localized mainly on the heteroatom of the nitrogen-containing heterocycle in the QR, while the positive charge is delocalized in the QB.

The formation of associates in solutions is more characteristic of dyes that have a flattened molecule geometry and developed  $\pi$ -electronic. Flattening enhances the component of noncovalent interactions due to the reduction of the distance between the corresponding fragments of interacting structures. Such properties have some squaraines,<sup>59–62</sup> spiropyrans,<sup>63,64</sup> porphyrins,<sup>65,66</sup> carbo- and merocyanines.<sup>67–70</sup> They are now being fruitfully studied in the processes of self- and heterogeneous association of dyes. But in contrast to similar structures, sulfonphthaleins (see also the structure of QB or QR in Table 1) are not flattened structures (see DBS, Table 1). However, the cation-anionic interactions for DBS are

expressed significantly as follows from the determined values of  $K_{as}$ . Based on experimental data on stoichiometry, it can be assumed that the cation coordinates with the single-charge DBS anion (or two cations coordinate with one double-charged DBS anion). Using quantum chemical simulations, we considered in more detail the energy state (value of the standard enthalpy of formation,  $\Delta_f H^0$ ) of each of the counterions and associates, and also determined their most probable structure.

### 3.3. Energy and structural properties of DBKS associates

The semi-empirical AM1 method as one of the extended variants of the MNDO method ("Modified Neglect of Diatomic Overlap") was used to estimate  $\Delta_f H^0$  ions and associates. The parameters of this method most correctly reproduce the experimental values of  $\Delta_f H^0$  of organic compounds. It should be noted that  $\Delta_f H^0$  calculations for organic molecules by non-empirical methods lead to errors exceeding 100 kJ/mol even for small molecules, while the average error of the AM1 method in calculating  $\Delta_f H^0$  is only 25 kJ/mol.<sup>71,72</sup> In advance, the geometry of all structures was optimized by the method of molecular mechanics MM+ (by the minimum value of the total energy  $E$ ). This significantly simplified the further determination of  $\Delta_f H^0$  by the semi-empirical method.

It is important to find the global energy minimum from a set of local minima to obtain the correct values of  $\Delta_f H^0$ . To do this, we tested from 3 to 5 different starting locations of counterions in the associate. From the received calculated set of energy minima the smallest was

chosen; the energy of this structure corresponded to the global energy minimum. For example, Fig. 7 shows three variants of the initial location of single-charged ions in the association of DBS with QB. Curve 3 corresponds to the variant with the energy of the global minimum  $E = 338$  kJ/mol.

Then additional geometric optimization of the associate structure was performed by setting several RMS-gradient values, which gradually decreased (the RMS gradient is the rate of energy change (the first derivative) when changing the location of each atom in three mutually perpendicular directions, kJ/(mol·Å)); the local minimum of the potential energy of a structure is considered reached when RMS = 0). The process of finding the optimized variant of the associate structure was considered complete when the value of  $\Delta_f H^0$  ceased to depend on the RMS values. This is indicated by the flatness of the area of the corresponding graphical dependence (Fig. 7; at  $RMS_{min} = 0.025$  the value of  $\Delta_f H^0$  is 311.7 kJ/mol). Table 3 shows the dependence of  $\Delta_f H^0$  on RMS values, as well as changes in the location of ions during the optimization process (the numbers on the dependence correspond to the location of dyes from the initial state (1) to the final one (5); stereo images are presented; the position of DBS (below) relative to the observer is conditionally fixed for clarity).

The process of structure optimization is accompanied by a decrease in the distance between the counterions (the distance between the ions along the axis 1 is from 7.3 Å (initial state 1) to 4.2 Å (final state 5), a certain deformation  $\pi$ -electronic dye systems and is almost finalized with a value of  $\Delta_f H^0 = 219.1$  kJ/mol at  $RMS_{min} = 0.025$ .

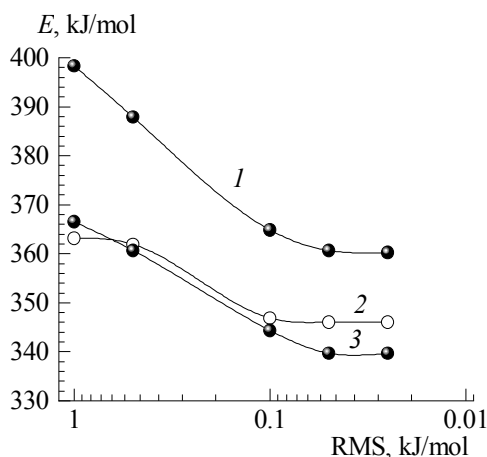


Fig. 7. Dependence of  $E$  on the RMS value for three variants (1–3) of different initial arrangement of ions in the associate of DBS with QB

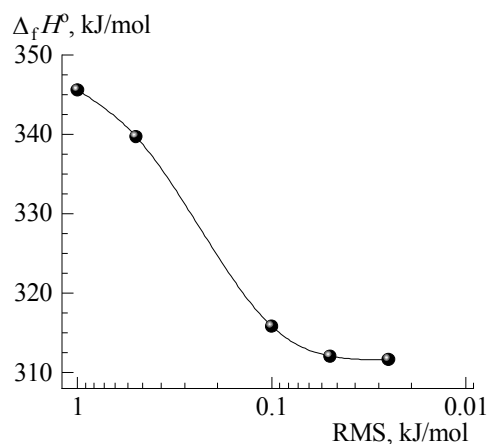
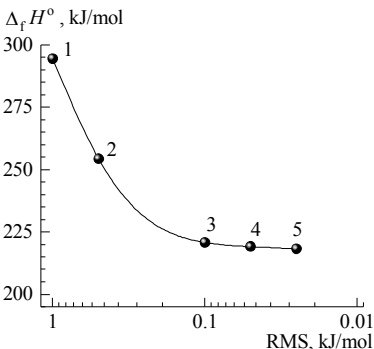
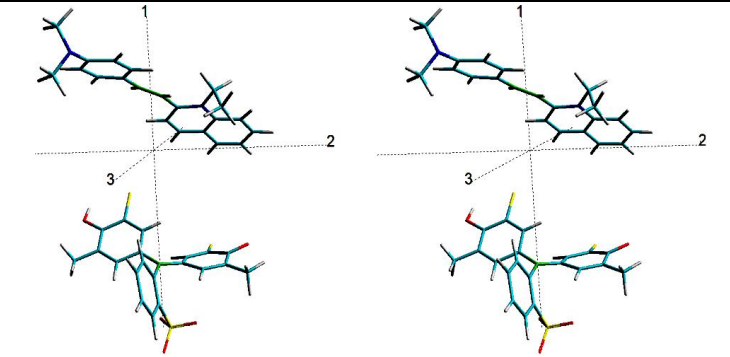
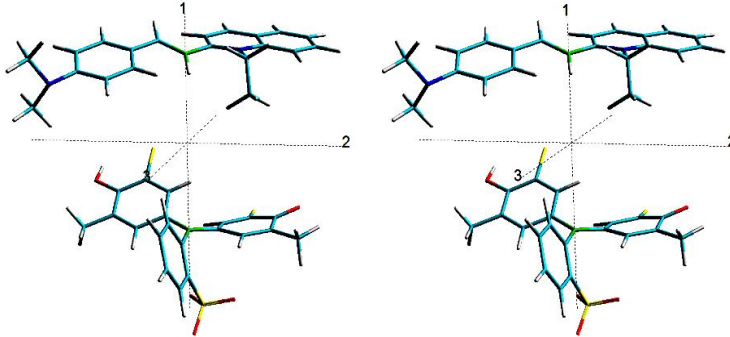
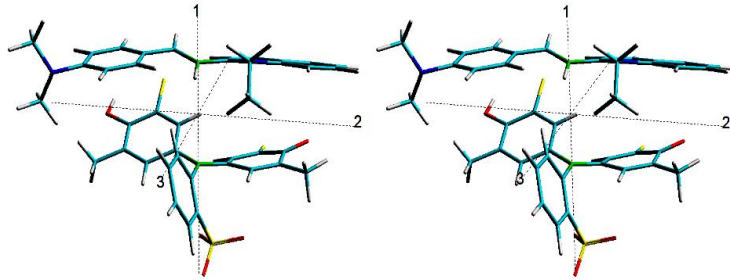
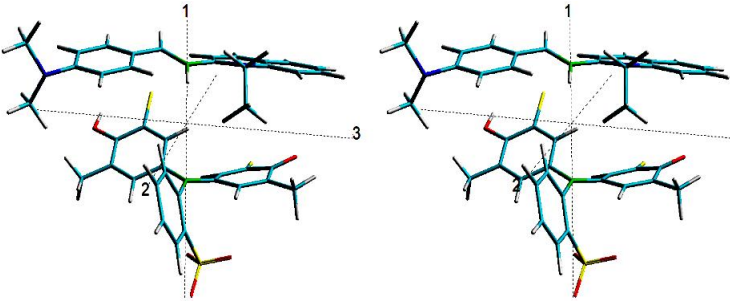
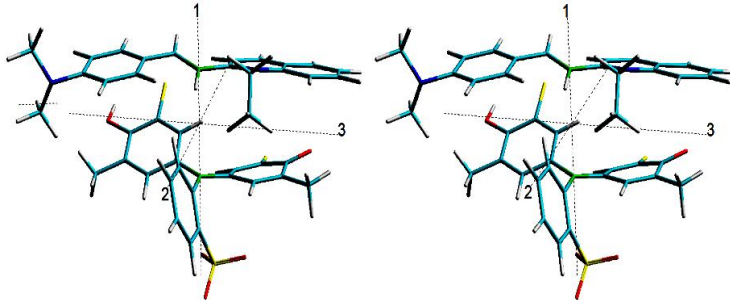


Fig. 8. Changes in  $\Delta_f H^0$  from RMS values for  $Ct^+ \cdot HAN^-$  an associate of DBS and QB dyes

**Table 3.** Dependence of  $\Delta_r H^\circ$  on RMS values and change of mutual arrangement of DBS and QR dyes in  $\text{Ct}^+ \cdot \text{HAN}^-$  associate

Dependence of $\Delta_r H^\circ$ on RMS values	State	Arrangement of DBS and QR in associate
	1	
	2	
	3	
	4	
	5	

We constructed energy diagrams of dye ions and their cation-anionic associates based on the calculations. The properties of the  $\text{HAN}^-$  associated with the  $\text{QR}$  cation are considered in Fig. 9 as an example (numbers near the arrows indicate the range of variation of the values of  $\Delta_f H^0$ , kJ/mol, for the corresponding particle). The values of  $\Delta_f H^0$  989...984 and -583...-602 kJ/mol correspond to  $\text{Ct}^+$  and  $\text{HAN}^-$  ions. Their algebraic sum  $\Sigma = 405.6...382.1$  kJ/mol (energy level 1) exceeds the value of  $\Delta_f H^0 = 220.8...219.1$  kJ/mol for the  $\text{Ct}^+\cdot\text{HAN}^-$  associate (level 2) by 186.5...161.3 kJ/mol. Similarly, we calculated the values  $\Delta_f H^0$  for all investigated associates (Table 4). In addition, Table 4 shows the values of  $\Sigma$  as the algebraic sum of the values  $\Delta_f H^0$  of the corresponding ions in the associate, which are defined as  $i \times \Delta_f H^0_f(\text{Ct}) + \Delta_f H^0_f(\text{An})$ , where  $i$  is the number of cations in the associate, and the relative error of the definition of  $\Delta_f H^0$ , which is calculated by the formula:

$$\delta = ((\mathbf{I}_{\max} - \mathbf{I}_{\min}) - (\mathbf{II}_{\min} - \mathbf{II}_{\max})) \times 100\% \times (\mathbf{I}_{\max} - \mathbf{II}_{\min})^{-1},$$

where  $\mathbf{I}_{\max}$  is the most value of  $i \times \Delta_f H^0_f(\text{Ct}) + \Delta_f H^0_f(\text{An})$ , kJ/mol,  $\mathbf{I}_{\min}$  is the smallest value of  $i \times \Delta_f H^0_f(\text{Ct}) + \Delta_f H^0_f(\text{An})$ , kJ/mol,  $\mathbf{II}_{\max}$  is the most value of  $\Delta_f H^0$  for an associate, kJ/mol,  $\mathbf{II}_{\min}$  is the smallest value of  $\Delta_f H^0$  for an associate, kJ/mol. The numerical values of  $\Sigma$ ,  $\Delta_f H^0$ ,  $\Sigma - \Delta_f H^0$  and the relative error  $\delta$  are given by integers; the  $\Delta_f H^0$  calculation error according to the above formula, which is additionally made by ignoring the decimal places does not exceed  $\pm 1$  kJ/mol.

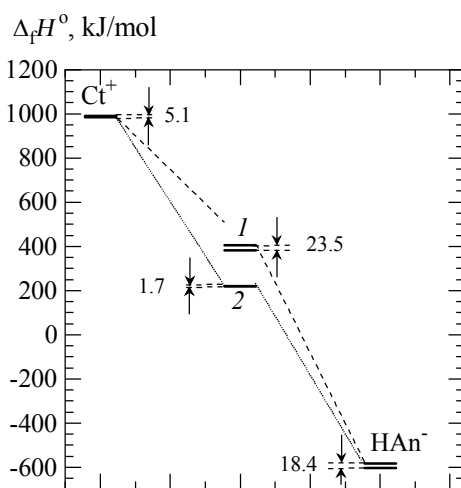


Fig. 9. The value of  $\Delta_f H^0$  for ions (QR, DBS) and the  $\text{Ct}^+\cdot\text{HAN}^-$  associate

Analysis of the results leads to an important conclusion. Since the error of the value of  $\Delta_f H^0$  does not exceed the average error of the method, we can assume that the formation of cation-anionic associations of DBS is energetically advantageous. Especially in the case of

association of DBS with a structure containing more developed  $\pi$ -electronic fragments ( $\text{QB}^+$ ). In addition, the value of  $\Delta_f H^0$  for associates of bromine-containing dyes is systematically higher in comparison with associates that do not contain bromine (cresolsulfonphthalein or thymolsulfonphthalein).<sup>44,48</sup> The bromine atoms, located in the plane of the benzene rings, have virtually no effect on the spatial structure of sulfonphthaleins, but significantly enhance the non-Coulomb component of intermolecular interactions. Thus, the introduction of halogen atoms into the structure of sulfonphthalein promotes the formation of cation-anionic associations between dyes.

Table 4. Values of  $\Delta_f H^0$  for DBS associates

Associate	$\Sigma$ , kJ/mol	$\Delta_f H^0_f$ , kJ/mol	$\Sigma \Delta_f H^0_f$ , kJ/mol / $\delta$ , %
$\text{QB}^+\cdot\text{DBS}^-$	471	312	159/29
$\text{QR}^+\cdot\text{DBS}^-$	382	219	163/13
$(\text{QB}^+)_2\cdot\text{DBS}^{2-}$	1590	928	662/4
$(\text{QR}^+)_2\cdot\text{DBS}^{2-}$	1411	737	674/7

## 4. Conclusions

The obtained results indicate that the processes of dye association are accompanied by a rather complex combination of different interactions, including non-Coulomb,  $\pi$ -electronic. The study of these processes is appropriate in terms of comparing the results of spectrophotometric measurements with computer simulation data. The interaction between single- or double-charged anions of DBS and cyanine cations at concentrations of particles  $5.0 \cdot 10^{-7} - 5.0 \cdot 10^{-5}$  mol/L has been investigated from the results of the spectrophotometric method and the semi-empirical method AM1. The optimal conditions have been revealed, under which the association is possible between counterions with stoichiometric ion ratios  $\text{Ct}^+ : \text{HAN}^- = 1 : 1$  and  $\text{Ct}^+ : \text{An}^{2-} = 2 : 1$ .

The association constants, as well as the standard enthalpies of formation of associates, energy diagrams, and the most probable structure of associates have been determined. Semi-empirical calculations are in agreement with the spectrophotometric data and indicate that the association of dye into an associate is possible and accompanied by a significant gain in energy. The study of the cation-anion association with the participation of DBS develops the idea of intermolecular interactions in solutions and creates a basis for further practical use of the spectral and equilibrium properties of the associates.

## References

- [1] Bishop, E. Observations on the Theory of Action of Visual Indicators. *Analyst* **1971**, *96*, 537-549. <https://doi.org/10.1039/AN9719600537>



- [2] Yamamoto, K.; Adachi, K. Interaction between Sulfonephthalein Dyes and Chitosan in Aqueous Solution and Its Application to the Determination of Surfactants. *Anal. Sci.* **2003**, *19*, 1133. <https://doi.org/10.2116/analsci.19.1133>
- [3] Shapovalov, S. *Association Processes with the Participation of Dyes in Solutions: Thermodynamic and Equilibrium Characteristics of Nanosystems*; LAP LAMBERT Academic Publishing: Riga, 2020.
- [4] Balderas-Hernández, P.; Ramírez-Silva, M.T.; Romero-Romo, M.; Palomar-Pardavé, M.; Roa-Morales, G.; Barrera-Díaz, C.; Rojas-Hernández, A. Experimental Correlation between the pKa Value of Sulfonphthaleins with the Nature of the Substituents Groups. *Spectrochim. Acta - A: Mol. Biomol. Spectrosc.* **2008**, *69*, 1235-1245. <https://doi.org/10.1016/j.saa.2007.06.038>
- [5] Ma, J.; Shu, H.; Yang, B.; Byrne, R.H.; Yuan, D. Spectrophotometric Determination of pH and Carbonate Ion Concentrations in Seawater: Choices, Constraints and Consequences. *Anal. Chim. Acta* **2019**, *1081*, 18-31. <https://doi.org/10.1016/j.aca.2019.06.024>
- [6] Hudson-Heck, E.; Liu, X.; Byrne, R.H. Purification and Physical-Chemical Characterization of Bromocresol Purple for Carbon System Measurements in Freshwaters, Estuaries, and Oceans. *ACS Omega* **2021**, *6*, 17941-17951. <https://doi.org/10.1021/acsomega.1c01579>
- [7] Takeshita, Y.; Warren, J.K.; Liu, X.; Spaulding, R.S.; Byrne, R.H.; Carter, B.R.; De Grandpre, M.D.; Murata, A.; Watanabe, S.-I. Consistency and Stability of Purified Meta-Cresol Purple for Spectrophotometric pH Measurements in Seawater. *Mar. Chem.* **2021**, *236*, 104018. <https://doi.org/10.1016/j.marchem.2021.104018>
- [8] Bargrizan, S.; Smernik, R.J.; Mosley, L.M. Development of a Spectrophotometric Method for Determining pH of Soil Extracts and Comparison with Glass Electrode Measurements. *Soil Sci. Soc. Am. J.* **2017**, *81*, 1350-1358. <https://doi.org/10.2136/sssaj2017.04.0119>
- [9] Bargrizan, S.; Smernik, R.J.; Fitzpatrick, R.W.; Mosley, L.M. The Application of a Spectrophotometric Method to Determine pH in Acidic (pH<5) Soils. *Talanta* **2018**, *186*, 421-426. <https://doi.org/10.1016/j.talanta.2018.04.074>
- [10] Bargrizan, S.; Smernik, R.J.; Mosley, L.M. Spectrophotometric Measurement of the pH of Soil Extracts Using a Multiple Indicator Dye Mixture. *Eur. J. Soil Sci.* **2019**, *70*, 411-420. <https://doi.org/10.1111/ejss.12745>
- [11] Jang, J.-S.; Kwon, S.-H. Micro pH Sensor Using Patterned Hydrogel with pH Indicator. *J. Sensor Sci. Technol.* **2011**, *20*, 234-237. <https://doi.org/10.5369/JSS.2011.20.4.234>
- [12] El Nahhal, I.M.; Zourab, S.M.; Kodeh, F.S.; Qudaih, A.I. Thin Film Optical BTB pH Sensors Using Sol-Gel Method in Presence of Surfactants. *Int. Nano Lett.* **2012**, *2*, 16. <https://doi.org/10.1186/2228-5326-2-16>
- [12] Tashyrev, O.B.; Sioma, I.B.; Tashyeva, G.O.; Hovorukha, V.M. Bromothymol Blue as the Universal Indicator for Determining the Stereometric Allocation of pH and Eh in the Medium in Heterophase Microorganisms Cultivation. *Mikrobiolohichnyi Zhurnal* **2019**, *81*, 14. <https://doi.org/10.15407/microbiolj81.02.014> (in Ukrainian)
- [13] Pinto, V.C.; Araújo, C.F.; Sousa, P.J.; Gonçalves, L.M.; Minas, G. A Low-Cost Lab-on-a-Chip Device for Marine pH Quantification by Colorimetry. *Sens. Actuators B Chem.* **2019**, *290*, 285-292. <https://doi.org/10.1016/j.snb.2019.03.098>
- [14] El-Nahhal, I.M.; Zourab, S.M.; Kodeh, F.S.; Abd el-Salam, F.H.; Baker, S.A. Sol-Gel Entrapment of Bromothymol Blue (BTB) Indicator in the Presence of Cationic 16E1Q and 16E1QS Surfactants. *J. Sol-Gel Sci. Technol.* **2016**, *79*, 628-636. <https://doi.org/10.1007/s10971-016-4044-x>
- [15] Kuswandi, B. Nanobiosensor Approaches for Pollutant Monitoring. *Environ. Chem. Lett.* **2019**, *17*, 975-990. <https://doi.org/10.1007/s10311-018-00853-x>
- [16] Mohamed, S.H.; Issa, Y.M.; Salim, A.I. Simultaneous Quantification of Simeprevir Sodium: A Hepatitis C Protease Inhibitor in Binary and Ternary Mixtures with Sofosbuvir and/or Ledipasvir Utilizing Direct and H-point Standard Addition Strategies. *Spectrochim. Acta - A: Mol. Biomol. Spectrosc.* **2019**, *210*, 290-297. <https://doi.org/10.1016/j.saa.2018.07.017>
- [17] Nguyen, T.D.; Le, H.B.; Dong, T.O.; Pham, T.D. Determination of Fluoroquinolones in Pharmaceutical Formulations by Extractive Spectrophotometric Methods Using Ion-Pair Complex Formation with Bromothymol Blue. *J. Anal. Methods Chem.* **2018**, *2018*, ID 8436948. <https://doi.org/10.1155/2018/8436948>
- [18] Issa, Y.M.; Abdel-Kader, N.S.; Zahran, A.E. Spectrophotometric Determination of Benzalkonium Chloride Using Sulfonphthaleins. *Int. J. Pharm. Sci. Rev. Res.* **2021**, *68*, 50-59. <http://dx.doi.org/10.47583/ijpsrr.2021.v68i01.009>
- [19] El-Ansary, A.L.; Abdel-Kader, N.S.; Asran, A.M. Spectrophotometric Studies on the Reaction of Diaveridine with Some Sulfonphthalein Dyes Based on Ion-Pair/Ion-Associate Complexes Formation. *J. Spectrosc. (Hindawi)* **2018**, *2018*, ID 9269148. <https://doi.org/10.1155/2018/9269148>
- [20] Antakli, S.; Nejem, L.; Ahmad, W.A. Determination of Flucloxacillin Sodium by Analytical Spectrophotometry. *Res. J. Pharm. Technol.* **2019**, *12*, 4757-4762. <https://doi.org/10.5958/0974-360X.2019.00820.5>
- [21] Gouda, A.A.; Hamdi, A.Y.; El Sheikh, R.; Abd Ellateif, A.E.; Badahdah, N.A.; Alzuhiri, M.E.; Saeed, E. Development and Validation of Spectrophotometric Methods for Estimation of Antimigraine Drug Eletriptan Hydrobromide in Pure Form and Pharmaceutical Formulations. *Ann. Pharm. Franç.* **2021**, *79*, 395-408. <https://doi.org/10.1016/j.pharma.2020.11.002>
- [22] Souri, E.; Amoon, E.; Ravari, N.S.; Keyghobadi, F.; Tehrani, M.B. Spectrophotometric Methods for Determination of Sunitinib in Pharmaceutical Dosage Forms Based on Ion-pair Complex Formation. *Iran J. Pharm. Res.* **2020**, *19*, 103-109. <https://doi.org/10.22037/ijpr.2020.1101119>
- [23] Cardoso, S.G.; Ieggli, C.V.S.; Pombum, S.C.G. Spectrophotometric Determination of Carvedilol in Pharmaceutical Formulations Through Charge-Transfer and Ion-Pair Complexation Reactions. *Pharmazie* **2007**, *62*, 34-37. <https://pubmed.ncbi.nlm.nih.gov/17294810>
- [24] Mohamed, S.H.; Issa, Y.M.; Elfeky, S.A. Extraction-Free Spectrophotometric Assay of the Antitussive Drug Pentoxifyverine Citrate Using Sulfonephthalein Dyes. *Spectrochim. Acta A. Mol. Biomol. Spectrosc.* **2019**, *222*, 117186. <https://doi.org/10.1016/j.saa.2019.117186>
- [25] Mohamed, S.H.; Issa, Y.M.; Elfeky, S.A.; Ahmed, A.A.; Abdel-Kader, N.S. Spectroscopic, Thermogravimetric Studies and DFT Calculations of Pentoxifyverine Citrate Ion-Pairs with Sulfonephthalein Dyes. *J. Mol. Struct.* **2020**, *1212*, 128074. <https://doi.org/10.1016/j.molstruc.2020.128074>
- [26] Alizadeh, N.; Keyhanian, F. Sensitive and Selective Spectrophotometric Assay of Piroxicam in Pure Form, Capsule and Human Blood Serum Samples via Ion-Pair Complex Formation. *Spectrochim. Acta A. Mol. Biomol. Spectrosc.* **2014**, *130*, 238-244. <https://doi.org/10.1016/j.saa.2014.03.074>
- [27] Kumar, A.; Singh, V.; Kumar, P. Spectrophotometric Estimation of Eflornithine Hydrochloride by Using Ion-Pair Reagents. *Pak. J. Pharm. Sci.* **2015**, *28*, 623-629. <https://pubmed.ncbi.nlm.nih.gov/25730793>

- [28] Mabrouk, M.M.; Gouda, A.A.; El-Malla, S.F.; Abdel Haleem, D.S. Sensitive Spectrophotometric Determination of Vardenafil HCl in Pure and Dosage Forms Détermination Spectrophotométrique Sensible du Vardénafil HCl Sous Formes Pures et Posologiques. *Ann. Pharm. Franç.* **2021**, *79*, 16-27. <https://doi.org/10.1016/j.pharma.2020.08.003>
- [29] Garg, B.; Bisht, T.; Ling, Y.-C. Colorimetric Recognition of Hydrazine in Aqueous solution by a Bromophenol Blue-Tethered Ion-pair-like Ratiometric Probe. *Spectrochim. Acta A. Mol. Biomol. Spectrosc.* **2021**, *251*, 119456. <https://doi.org/10.1016/j.saa.2021.119456>
- [30] van de Logt, A.-E.; Rijpmma, S.R.; Vink, C.H.; Prudon-Rosmulder, E.; Wetzels, J.F.; van Berkel, M. The Bias between Different Albumin Assays May Affect Clinical Decision-Making. *Kidney Int.* **2019**, *95*, 1514-1517. <https://doi.org/10.1016/j.kint.2019.01.042>
- [31] Zeybek, D.K.; Demir, B.; Zeybek, B.; Pekyardımcı, P. A Sensitive Electrochemical DNA Biosensor for Antineoplastic Drug 5-Fluorouracil Based on Glassy Carbon Electrode Modified with Poly(Bromocresol Purple). *Talanta* **2015**, *144*, 793-800. <https://doi.org/10.1016/j.talanta.2015.06.077>
- [32] Aljerf, L. High-Efficiency Extraction of Bromocresol Purple Dye and Heavy Metals as Chromium from Industrial Effluent by Adsorption onto a Modified Surface of Zeolite: Kinetics and equilibrium study. *J. Environ. Manage* **2018**, *225*, 120-132. <https://doi.org/10.1016/j.jenvman.2018.07.048>
- [33] Kim, Y.H.; Sathiyarayanan, G.; Kim, H.J.; Bhatia, S.K.; Seo, H.-M.; Kim, J.-H.; Song, H.-S.; Kim, Y.-G.; Park, K.; Yang, Y.-H. A Liquid-Based Colorimetric Assay of Lysine Decarboxylase and Its Application to Enzymatic Assay. *J. Microbiol. Biotechnol.* **2015**, *25*, 2110-2115. <https://doi.org/10.4014/jmb.1505.05063>
- [34] Zeng, J.; Eckenrode, H.M.; Dai, H.-L.; Wilhelm, M.J. Adsorption and Transport of Charged vs. Neutral Hydrophobic Molecules at the Membrane of Murine Erythroleukemia (MEL) Cells. *Colloids Surf. B: Biointerfaces* **2015**, *127*, 122-129. <https://doi.org/10.1016/j.colsurfb.2015.01.014>
- [35] Thompson, S.; Ding, L.-E. Underestimation of the Serum Ascites Albumin Gradient by the Bromocresol Purple Method of Albumin Measurement. *Intern. Med. J.* **2018**, *48*, 1412-1413. <https://doi.org/10.1111/imj.14101>
- [36] Garcia Moreira, V.; Beridze Vaktangova, N.; Martinez Gago, M.D.; Laborda Gonzalez, B.; Garcia Alonso, S.; Fernandez Rodriguez, E. Overestimation of Albumin Measured by Bromocresol Green vs Bromocresol Purple Method: Influence of Acute-Phase Globulins. *Lab. Med.* **2018**, *49*, 355-361. <https://doi.org/10.1093/labmed/lmy020>
- [37] Le Reun, E.; Leven, C.; Lapègue, M.; Kerspern, H.; Rouillé, A.; Labarre, M.; Carré, J.-L.; Padelli, M. Assessment of Immunoturbidimetric DiAgam Kit for Plasma Albumin Measurement: A Comparative Study. *Ann. Biol. Clin. (Paris)* **2018**, *76*, 477-479. <https://doi.org/10.1684/abc.2018.1361d>
- [38] Delanghe, S.; Van Biesen, W.; Van de Velde, N.; Eloot, S.; Pletinck, A.; Schepers, E.; Glorieux, G.; Delanghe, J.R.; Speeckaert, M.M. Binding of Bromocresol Green and Bromocresol Purple to Albumin in Hemodialysis Patients. *Clin. Chem. Lab. Med.* **2018**, *56*, 436. <https://doi.org/10.1515/cclm-2017-0444>
- [39] Pan, W.C.; Lau, W.; Mattman, A.; Kiaii, M.; Jung, B. Comparison of Hypoalbuminemia-Corrected Serum Calcium Using BCP Albumin Assay to Ionized Calcium and Impact on Prescribing in Hemodialysis Patients. *Clin. Nephrol.* **2018**, *89*, 34-40. <https://doi.org/10.5414/CN109070>
- [40] Ueno, T.; Hirayama, S.; Sugihara, M.; Miida, T. The Bromocresol Green Assay, but not the Modified Bromocresol Purple Assay, Overestimates the Serum Albumin Concentration in Nephrotic Syndrome through Reaction with  $\alpha$ 2-Macroglobulin. *Ann. Clin. Biochem.* **2016**, *53*, 97. <https://doi.org/10.1177/0004563215574350>
- [41] Yoshihiro, S.; Ishigaki, T.; Ookurano, H.; Yoshitomi, F.; Hotta, T.; Kang, D.; Hokazono, E.; Kayamori, Y. New Colorimetric Method with Bromocresol Purple for Estimating the Redox State of Human Serum Albumin. *J. Clin. Biochem. Nutr.* **2020**, *67*, 257-262. <https://doi.org/10.3164/jcbrn.20-10>
- [42] Chmelová, D.; Ondrejovič, M. Purification and Characterization of Extracellular Laccase Produced by *Ceriporiopsis Subvermispora* and Decolorization of Triphenylmethane Dyes. *J. Basic Microbiol.* **2016**, *56*, 1173-1182. <https://doi.org/10.1002/jobm.201600152>
- [43] Shapovalov, S.A.; Koval, V.L.; Chernaya, T.A.; Pereverzev, A.Yu.; Derevyanko, N.A.; Ishchenko, A.A.; Mchedlov-Petrosyan, N.O. Association of Indopolymethine Cyanine Cations with Anions of Sulfonephthalein and Xanthene Dyes in Water. *J. Brazil. Chem. Soc.* **2005**, *16*, 232. <https://doi.org/10.1590/S0103-50532005000200017>
- [44] Shapovalov, S.; Kiseliova, Ya. Association of Thymolsulfonephthalein and Cresolsulfonephthalein Anions with Cationic Cyanines in Aqueous Solution. *Chem. Chem. Technol.* **2010**, *4*, 271-276. <https://doi.org/10.23939/chcht04.04.271>
- [45] Shapovalov, S. Association of Quinaldine Red Cation in an Aqueous Solution: The Interaction with Anionic Dyes. *AASCTT Journal of Nanoscience* **2018**, *3*, 35-40.
- [46] Shapovalov, S.; Kiseliova, Ya. Heteroassociation of the Bromine-Containing Anions of Sulfophthaleins in Aqueous Solution. *Russ. Chem. Bull.* **2010**, *59*, 1317-1326. <https://doi.org/10.1007/s11172-010-0241-x>
- [47] Šapovalov, S.; Samojlov, E.; Yvanov, V. *Chymyja i chym. tehnolohyja* **2006**, *49*, 39-44.
- [48] Shapovalov, S. Association of Anions of Phenolsulfonephthalein and its Alkyl-Substituted Derivatives with Single-Charged Cations of Polymethines. *Russ. Chem. Bull.* **2011**, *60*, 465. <https://doi.org/10.1007/s11172-011-0073-3>
- [49] Gupta, D.; Read, J. First pKa Values of Some Acid-Base Indicators. *J. Pharm. Sci.* **1970**, *11*, 1683-1685. <https://doi.org/10.1002/jps.2600591136>
- [50] Herz, A. *Photogr. Sci. Eng.* **1974**, *18*, 207-215.
- [51] Savitzky, A.; Golay, M.J.E. Smoothing and Differentiation of Data by Simplified Least Squares Procedures. *Anal. Chem.* **1964**, *36*, 1627-1639. <https://doi.org/10.1021/ac60214a047>
- [52] Paris, Q. The Dual of the Least-Squares Method. *Open J. Statist.* **2015**, *5*, 658-664. <https://doi.org/10.4236/ojs.2015.57067>
- [53] Shapovalov, S.; Samoilov, E. Regularities of Homo- and Heteroassociation of the Pinacyanone Cation in Aqueous Solution. *Russ. Chem. Bull.* **2008**, *57*, 1405-1415. <https://doi.org/10.1007/s11172-008-0183-8>
- [54] Ishchenko, A.; Shapovalov, S. Heterogeneous Association of the Ions of Dyes in Solutions (Review). *J. Appl. Spectrosc.* **2004**, *71*, 605-629. <https://doi.org/10.1023/B:JAPS.0000049618.42857.0a>
- [55] Šapovalov, S.; Svyščeva, Ja. *Visnyk Charkiv. Nacionaln. Un-tu. Chymija* **2000**, *477*, 112. (in Ukrainian)
- [56] Veselkov, D.; Evstyhneev, M.; Kodynceev, V. *Žurn. fizyč. chymyja* **2001**, *75*, 879.
- [57] Veselkov, D.; Syhaev, V.; Vysockyj, S. *Žurn. strukt. chymyja* **2000**, *41*, 86.
- [58] Šapovalov, S. *Ukr. chymyč. žurn.* **2004**, *70*, 25.
- [59] Martins, T.D.; Pacheco, M.L.; Boto, R.E.; Almeida, P.; Farinha, J.P.S.; Reis, L.V. Synthesis, Characterization and Protein-Association of Dicyanomethylene Squaraine Dyes. *Dyes Pigm.*

- 2017, 147, 120-129. <https://doi.org/10.1016/j.dyepig.2017.07.070>
- [60] Barbero, N.; Butnarasu, C.; Visentin, S.; Barolo, C. Squaraine Dyes: Interaction with Bovine Serum Albumin to Investigate Supramolecular Adducts with Aggregation-Induced Emission (AIE) Properties. *Chem. Asian J.* **2019**, *14*, 896-903. <https://doi.org/10.1002/asia.201900055>
- [61] Hovor, I.V.; Fedyunyayeva, I.A.; Obukhova, O.M.; Kolosova, O.S.; Tatarets, A.L. Zastosuvannya Styryloвого ta Skvarainovogo Barvnykiv dla Vyznachennya Konformatsiinykh Zmin u Molekulakh Proteiniv. *Odesa National University Herald. Chemistry* **2020**, *25*, 94. [https://doi.org/10.18524/2304-0947.2020.3\(75\).212477](https://doi.org/10.18524/2304-0947.2020.3(75).212477) (in Ukrainian)
- [62] Iliina, K.; MacCuaig, W.M.; Laramie, M.; Jeouty, J.N.; McNally, L.R.; Henary, M. Squaraine Dyes: Molecular Design for Different Applications and Remaining Challenges. *Bioconjugate Chem.* **2020**, *31*, 194-213. <https://doi.org/10.1021/acs.bioconjchem.9b00482>
- [63] Kortekaas, L.; Browne, W.R. The Evolution of Spiropyran: Fundamentals and Progress of an Extraordinarily Versatile Photochrome. *Chem. Soc. Rev.* **2019**, *48*, 3406-3424. <https://doi.org/10.1039/C9CS00203K> - <https://pubs.rsc.org/en/content/articlelanding/2019/cs/c9cs00203k>
- [64] Zhang, Y.; Ng, M.; Chan, M.H.-Y.; Wu, N.M.-W.; Wu, L.; Yam, V.W.-W. Synthesis and Characterization of Photochromic Triethylene Glycol-Containing Spiropyrans and their Assembly in Solution. *Org. Chem. Front.* **2021**, *8*, 3047-3058. <https://doi.org/10.1039/D1QO00316J>
- [65] Zurita, A.; Duran, A.; Ribó, J.M.; El-Hachemi, Z.; Crusats, J. Hyperporphyrin Effects Extended into a J-Aggregate Supramolecular Structure in Water. *RSC Adv.* **2017**, *7*, 3353-3357. <https://doi.org/10.1039/C6RA27441B>
- [66] Gaeta, M.; Sortino, G.; Randazzo, R.; Pisagatti, I.; Notti, A.; Fragalà, M.E.; Parisi, M.F.; D'Urso, A.; Purrello, R. Long-Range Chiral Induction by a Fully Noncovalent Approach in Supramolecular Porphyrin-Calixarene Assemblies. *Chem. Eur. J.* **2020**, *26*, 3515-3318. <https://doi.org/10.1002/chem.202000126>
- [67] Pronkin, P.G.; Tatikolov, A.S. Formation of J-Aggregates of an Anionic Oxacarbocyanine Dye Upon Interaction with Proteins and Polyelectrolytes. *J. Appl. Spectrosc.* **2017**, *84*, 217-224. <https://doi.org/10.1007/s10812-017-0454-y>
- [68] Bricks, J.L.; Slominskii, Y.L.; Panas, I.D.; Demchenko, A.P. Fluorescent J-Aggregates of Cyanine Dyes: Basic Research and

- Applications Review. *Methods Appl. Fluoresc.* **2017**, *6*, 012001. <https://doi.org/10.1088/2050-6120/aa8d0d>
- [69] Nordhaus, M.A.; Krongauz, V.V.; Hai, T.T. Synthesis of Solvatochromic Merocyanine Dyes and their Immobilization to Polymers. *J. Appl. Polym. Sci.* **2017**, *134*, 44451. <https://doi.org/10.1002/app.44451>
- [70] Pasch, P.; Papadopoulos, J.; Goralczyk, A.; Hofer, M.L.; Tabatabai, M.; Müller, T.J.J.; Hartmann, L. Highly Fluorescent Merocyanine and Cyanine PMMA Copolymers. *Macromol. Rapid Comm.* **2018**, *39*, 1800277. <https://doi.org/10.1002/marc.201800277>
- [71] Dewar, M.J.S.; Storch, D.M. Development and Use of Quantum Molecular Models. 75. Comparative Tests of Theoretical Procedures for Studying Chemical Reactions. *J. Am. Chem. Soc.* **1985**, *107*, 3898-3902. <https://doi.org/10.1021/ja00299a023>
- [72] Stewart, J.J.P. Optimization of Parameters for Semiempirical Methods I. Method. *J. Comput. Chem.* **1989**, *10*, 209-220. <https://doi.org/10.1002/jcc.540100208>

Received: June 17, 2021 / Revised: August 21, 2021 / Accepted: September 27, 2021

### АСОЦІАЦІЯ АНІОНІВ 5,5'-ДИБРОМО-О-КРЕЗОЛСУЛЬФОНФТАЛЕЇНУ З КАТІОНАМИ БАРВНИКІВ У ВОДНОМУ РОЗЧИНІ

**Анотація.** Розглянуто утворення у водному розчині асоціатів між одно- або двозарядними аніонами 5,5'-дибромом-о-крезолсульфонфталейну й однозарядними катіонами ціанінових барвників (квінальдиновий синій, квінальдиновий червоний). На підставі спектروفотометричних даних проаналізовані значення рівноважних констант асоціації. Непівемпіричним квантовохімічним методом АМ1 визначена енергетика катіон-аніонних взаємодій (стандартна ентальпія утворення іонів та асоціатів) і встановлена ймовірна будова асоціатів. Обговорена узгодженість між експериментальними спектروفотометричними та розрахунковими квантовохімічними даними.

**Ключові слова:** асоціація, спектри поглинання, 5,5'-дибромом-о-крезолсульфонфталейн, барвники, ентальпія утворення, метод АМ1.